

A Mechanism for Tamoxifen-mediated Inhibition of Acidification*

(Received for publication, February 25, 1999)

Yu Chen^{‡§}, Melvin Schindler^{¶||}, and Sanford M. Simon^{‡**}

From the [‡]Laboratory of Cellular Biophysics, Rockefeller University, New York, New York 10021
and the [¶]Department of Biochemistry, Michigan State University, East Lansing, Michigan 48824

Tamoxifen has been reported to inhibit acidification of cytoplasmic organelles in mammalian cells. Here, the mechanism of this inhibition is investigated using *in vitro* assays on isolated organelles and liposomes. Tamoxifen inhibited ATP-dependent acidification in organelles from a variety of sources, including isolated microsomes from mammalian cells, vacuoles from *Saccharomyces cerevisiae*, and inverted membrane vesicles from *Escherichia coli*. Tamoxifen increased the ATPase activity of the vacuolar proton ATPase but decreased the membrane potential (V_m) generated by this proton pump, suggesting that tamoxifen may act by increasing proton permeability. In liposomes, tamoxifen increased the rate of pH dissipation. Studies comparing the effect of tamoxifen on pH gradients using different salt conditions and with other known ionophores suggest that tamoxifen affects transmembrane pH through two independent mechanisms. First, as a lipophilic weak base, it partitions into acidic vesicles, resulting in rapid neutralization. Second, it mediates coupled, electroneutral transport of proton or hydroxide with chloride. An understanding of the biochemical mechanism(s) for the effects of tamoxifen that are independent of the estrogen receptor could contribute to predicting side effects of tamoxifen and in designing screens to select for estrogen-receptor antagonists without these side effects.

Tamoxifen is the most commonly used treatment for breast cancer (1). In addition, it is currently being considered for widespread use in healthy women for breast cancer prevention (2, 3). Yet, despite its widespread use, its mechanisms of action remain obscure. Tamoxifen is a known estrogen receptor modulator that acts as an antagonist or partial agonist. But it has also been reported to have many pleiotropic effects both *in vivo* and *in vitro* that cannot be explained by an interaction with the estrogen receptor (4). For example, tamoxifen has been shown to enhance drug sensitivity of multidrug-resistant cells (5–9), inhibit bone resorption and osteoporosis both *in vivo* and *in vitro* (10), and inhibit a number of channels, including the volume activated chloride channel (11, 12) and calcium channels (13–16). These effects have been attributed to inhibition of

P-glycoprotein (17), calmodulin (15), and direct channel interaction (11), respectively.

Previously, we have observed that tamoxifen inhibits acidification of intracellular organelles of both estrogen receptor positive and negative cell lines (18). This inhibition of acidification may be a mechanism for many of the effects of tamoxifen. For example, the effects of tamoxifen on osteoporosis (19), vesicular transport (20, 21), or multidrug resistance (9, 22) are mimicked by blocking the proton vATPase¹ or by a protonophore.

This work addresses the mechanism(s) by which tamoxifen inhibits ATP-dependent *in vitro* acidification of organelles isolated from tissue culture cells, whole tissue, vacuoles from *Saccharomyces cerevisiae*, and inverted vesicles isolated from *Escherichia coli*. The studies on yeast vacuolar acidification demonstrate that tamoxifen decreased both ATP-generated pH gradients and V_m but increased the ATPase activity of the vATPase. These results suggest that tamoxifen affects ion permeability of a variety of biological membranes through interaction with either membrane proteins or the lipid bilayer.

The possibility that tamoxifen acts directly on the lipid bilayer was addressed with studies of pure lipid vesicles in which tamoxifen increased the rate of dissipation of the pH gradient. The data suggest that this occurs by two distinct mechanisms. First, tamoxifen is a lipophilic weak base with a neutral form that can readily flip-flop between membranes, and a basic form that is relatively impermeable. Thus, tamoxifen would accumulate in acidic vesicles, bind protons, and increase luminal pH. Importantly, tamoxifen is over 1000-fold more potent in increasing luminal pH than the soluble weak base ammonium chloride. This may be explained by the predominant partitioning of tamoxifen into the lipid phase, increasing the effective concentration. However, this mechanism can only be involved in dissipation of a pH gradient when the lumen is acidic. Second, tamoxifen can mediate coupled transport of proton or hydroxide with chloride based on the following observations: 1) it mediates electroneutral dissipation of pH gradients that is dependent on the presence of chloride or other halides; 2) it mediates an increased dissipation rate of chloride gradients; 3) it mediates net proton influx when the external chloride concentration is greater than the luminal chloride concentration.

Acidification is crucial for the proper functioning of many cellular processes, and its disruption may account for many of the pleiotropic effects described for tamoxifen. The results presented here show that at low micromolar concentrations, tamoxifen can inhibit acidification and dissipate pH gradients in a variety of *in vitro* systems, supporting *in vivo* data (18). Whereas this concentration is higher than required to modu-

* This work was supported in part by American Chemical Society Grant RPG-98-177-01-CDD and National Institutes of Health Grant R01CA81257 (to S. M. S.). The costs of publication of this article were defrayed in part by the payment of page charges. This article must therefore be hereby marked "advertisement" in accordance with 18 U.S.C. Section 1734 solely to indicate this fact.

§ Supported by National Institutes of Health Grant MSTP GM07739 at the Cornell/Rockefeller/Sloan Kettering Tri-institutional M.D./Ph.D. program.

|| Supported by the Pardee Foundation (Midland, MD).

** Supported by the Wolfensohn Foundation. To whom correspondence should be addressed: Laboratory of Cellular Biophysics, Rockefeller University, 1230 York Ave., New York, NY 10021. Tel.: 212-327-8130; Fax: 212-327-8022; E-mail: simon@rockvax.rockefeller.edu.

¹ The abbreviations used are: vATPase, vacuolar ATPase; AO, acridine orange; DPX, *p*-xylene-bispyridinium bromide; POPC, palmitoyloleoyl phosphatidylcholine; DTT, dithiothreitol; FITC, fluorescein isothiocyanate; Tricine, *N*-[2-hydroxy-1,1-bis(hydroxymethyl)ethyl]glycine; MES, 4-morpholineethanesulfonic acid; MOPS, 4-morpholinepropanesulfonic acid; FCCP, carbonyl cyanide *p*-trifluoromethoxyphenylhydrazone; InV, inverted vesicles.

late the estrogen receptor, it is similar to those reported for many estrogen receptor independent effects. Importantly, this concentration can readily be achieved in the clinic. The elucidation of a biochemical mechanism for this estrogen receptor independent activity of tamoxifen could significantly contribute to the design of modulators of the estrogen receptor that lack these side effects.

EXPERIMENTAL PROCEDURES

Materials—Bafilomycin A₁, monensin, acridine orange (AO), pyranine (8-hydroxypyrene-1,3,6-trisulfonic acid), tamoxifen, Tris-ATP, and nigericin were from Sigma. BODIPY®-transferrin, lucigenin, and *p*-xylylene-bispyridinium bromide (DPX) were from Molecular Probes (Eugene, OR). Adriamycin was from Calbiochem. Concanamycin A was from Fluka (Milwaukee, WI). Palmitoyloleoyl phosphatidylcholine (POPC) and cholesterol were from Avanti Polar Lipids (Alabaster, AL).

Acidification of Cellular Microsomes—Cells were grown in minimal essential medium supplemented with 10% fetal bovine serum to confluence in 10-level cell factories (Nunc, Naperville, IL), trypsinized, washed 3× with cold phosphate-buffered saline, and lysed with a Dounce homogenizer (pestle A) in 0.25 M sucrose, 20 mM HEPES, pH 7.4, 1 mM DTT, 1 mM EDTA, and 1× protease inhibitor mix (1 μg/ml leupeptin, 1 μg/ml pepstatin A, 1 μg/ml aprotinin, and 16 μM phenylmethylsulfonyl fluoride mixed to 100× before use). The homogenate was centrifuged twice for 10 min at 3000 × *g* to remove unbroken cells and nuclei. The supernatant was layered over 20 ml of 0.5 M sucrose (20 mM HEPES, pH 7.4, 1 mM DTT, 1 mM EDTA, 1× protease inhibitor mix) and 1 ml of 2 M sucrose and centrifuged for 1 h at 100,000 × *g* (Beckman Ti60 Rotor). Microsomes are collected at the 0.5 and 2 M interface.

To monitor acidification of the total microsomal fraction, the quenching of AO fluorescence was monitored essentially as described previously (23). Acidic vesicles accumulate AO to high concentrations resulting in the self-quenching of the dye and a decrease of the overall fluorescence. Fluorescence was measured on an SLM Aminco-Bowman series 2 luminescence spectrometer with $\lambda_{\text{ex}} = 488$ nm and $\lambda_{\text{em}} = 530$ nm. Microsomes (80 μg of protein) were suspended in 2.5 ml of vesicle buffer (125 mM KCl, 5 mM MgCl₂, 20 mM HEPES, pH 7.4, 1 mM DTT, 1 mM EDTA, 2 mM Na₂S₂O₃), with 6 μM AO (5 mM stock in H₂O) in a cuvette. To examine the ability of vesicles to generate a ΔpH in the presence of tamoxifen or bafilomycin A₁, 0, 1, 2, 4, or 8 μM tamoxifen (10 mM stock in EtOH) or 10 nM bafilomycin A₁ (10 mM stock in 10% Me₂SO) was added. After equilibration for 30 min at 25 °C, 1 mM Tris-ATP was added to begin acidification (100 mM stock, titrated to pH 7.4 with 1 M Tris base before use). Twenty minutes later, 2.5 μM nigericin (10 mM stock in EtOH) was added to dissipate any ΔpH formation. To study the effects of tamoxifen and bafilomycin A₁ on vesicles with a pre-existing ΔpH tamoxifen or bafilomycin A₁ were added 10 min after the addition of Tris-ATP.

Acidification from the recycling endosomal fraction was monitored by first incubating cells with FITC-transferrin for 30 min before lysis and isolation of microsomes. Acidification was monitored by excitation of the FITC fluorophore at 450 and 488 nm and measuring $\lambda_{\text{em}} = 520$ nm as described previously (18).

Acidification of Yeast Vacuoles—Vacuoles from *S. cerevisiae* were prepared from the protease-deficient strain BJ2407 (Yeast Genetic Stock Center, University of California, Berkeley) by sequential flotation through 12 and 8% Ficoll 400 cushion as described previously (24) with the single modification that 1× protease inhibitor mix and 1 mM DTT was included in each step. This procedure produced a 25-fold enrichment of the vacuolar marker α-mannosidase (data not shown). Acidification was measured using AO as described above. For acidification in chloride-free solution, gluconate or glutamate was used in vesicle buffer instead of chloride.

Acidification of *E. coli* Inverted Membrane Vesicles—InV were prepared from the DH5α strain as described (25). Acidification was measured using AO as described above.

V_m of Yeast Vacuoles—Oxonol V is a membrane-permeable anionic fluorescent probe that accumulates into the inner leaflet of vesicles with positive V_m, resulting in quenching of fluorescence. Vacuoles were suspended in chloride or gluconate vesicle buffer with 1 μM oxonol V. Fluorescence was measured with a $\lambda_{\text{ex}} = 600$ nm and $\lambda_{\text{em}} = 630$ nm. After fluorescence had equilibrated, vacuoles were added, and the fluorescence was allowed to re-equilibrate. Then, 1 mM Tris-ATP was added, and the resulting positive V_m was manifested in fluorescence quenching.

ATPase Activity of Yeast vATPase—Vacuoles were diluted in KCl or potassium gluconate vesicle buffer. Each sample was split into two, and

either 5 μM tamoxifen or carrier was added. Each of the four resulting samples was again split into two, and either carrier or 100 nM bafilomycin A₁ was added. Next, 2 mM Tris-ATP was added to each sample, and the vacuoles were incubated at 30 °C for 15 min. To measure the phosphate concentration from ATP hydrolysis, an equal volume of Taussky-Shorr Reagent (1% w/v ammonium molybdate, 2.7% v/v sulfuric acid, and 5% w/v ferrous sulfate hexahydrate) was added, and the samples were developed for 15 min. The A₆₆₀ was measured (Spectronic Genesys 2) which is linearly related to phosphate concentration. The bafilomycin-inhibitable ATPase activity was taken as the difference between the ATPase activity of each condition with or without 100 nM bafilomycin A₁.

Liposome pH—The luminal pH (pH_L) of liposomes was assayed with pyranine, a fluorescent dye with a pK_a ~7.3 and a $\lambda_{\text{ex}} = 405$ nm in its acid form (−3 charge) and a $\lambda_{\text{ex}} = 455$ nm in its basic form (−4 charge). To prepare pyranine-loaded liposomes, lipids (2 mg of POPC, 1 mg of cholesterol) supplied in chloroform suspension were dried in a round bottom flask under argon for 2 h. The lipids were then resuspended in acidic or alkaline liposome buffer (300 mM KCl, 20 mM MES, 20 mM MOPS, 20 mM Tricine titrated with KOH to either pH 6.2 or pH 8.1) containing 0.5 mM pyranine. The suspension was incubated at room temperature overnight and then freeze-thawed 6 times. Unilamellar liposomes were prepared by extrusion 3 times through two stacked 100-nm Nucleopore (Corning/Costar Scientific, Acton, MA) polycarbonate filters in an Avestin (Vancouver, British Columbia, Canada) extruder at 600 pounds/square inch. More than 95% of external pyranine was separated from the liposomes by sequentially running through NAP-10 and NAP-25 desalting columns (Amersham Pharmacia Biotech). Internal pyranine leakage was <1% per day, and liposomes were used within 1 week of preparation.

The pyranine fluorescence was calibrated as a function of pH by diluting the liposomes with pH 6.2 into a weakly buffered solution of identical pH (300 mM KCl, 1 mM MES, 1 mM MOPS, 1 mM Tricine, pH 6.2), 1 μM nigericin to allow rapid equilibration with external pH, and 5 mM DPX to quench external pyranine. The ratio of the fluorescence emission at $\lambda_{\text{em}} = 510$ nm was monitored with dual excitation wavelengths of $\lambda_{\text{ex}} = 405$ and $\lambda_{\text{ex}} = 455$ nm. Sequential aliquots of 0.1 mM glycylglycine, pH 8.4, were added to increase pH (see Fig. 5). The fluorescence was measured after each addition, and the pH was measured using a pH meter. The logarithm of the fluorescence ratio was linearly dependent on the pH. The curve generated by a least squares fit between pH 6.2 and 7.9 resulted in $\chi^2 > 0.99$. The calibration curve for the liposomes of luminal pH 8.1 was generated identically except sequential aliquots of 0.1 mM K-MES, pH 5.0, were added for titration, and the curve was generated between pH 8.1 and pH 6.4.

To measure the rate of pH dissipation of liposomes with luminal pH 6.2, the liposomes were diluted in weakly buffered solution of identical pH as described above but with no nigericin. Various agents (tamoxifen, valinomycin, and FCCP) were included as described in the text. The external pH was shifted to pH 7.3 by addition of 5 mM glycylglycine, pH 8.4, and the fluorescence ratio was monitored. After 10 min, 1 μM nigericin was added to dissipate the remaining pH gradient. The pH_L was calculated using the equation $\text{pH} = x \cdot \log(\lambda_{\text{ex}} = 405 \text{ nm} / \lambda_{\text{ex}} = 405 \text{ nm}) + c$, where *x* and *c* are constants from the least square fit of the titration curve. To measure the rate of pH dissipation of liposomes with pH_L = 8.1, the identical procedure was followed except 5 mM K-MES, pH 5.0, was added to shift the external pH to 6.9.

To assay the effect of addition of NH₄Cl or tamoxifen on liposome pH, liposomes with pH_L = 6.2 were diluted into identical buffer (300 mM KCl, 20 mM MES, 20 mM MOPS, 20 mM Tricine, pH 6.2) containing 5 mM DPX, and the fluorescence ratio was followed after addition of NH₄Cl or tamoxifen.

Liposome Chloride Concentration—Lucigenin is a fluorescent dye that is collisionally quenched by chloride and other halides but not by nitrate (26). Lipids dried as described above were rehydrated in 300 mM KNO₃, 10 mM K-HEPES, pH 7.3, and 0.5 mM lucigenin. 100 nM unilamellar liposomes were made, and external dye was removed as described above.

To calibrate the fluorescence of lucigenin as a function of chloride, the liposomes were diluted in buffer (300 mM KNO₃, 10 mM K-HEPES, pH 7.3) with 1 μM tributyltin (TBT) a Cl[−]-OH[−] exchanger, and 1 μM nigericin, a K⁺-H⁺ exchanger. This results in rapid net dissipation of KCl gradient. Aliquots of 0.5, 1, 2, 4, 8, 16, and 32 mM KCl were added, and lucigenin fluorescence ($\lambda_{\text{ex}} = 370$ nm/ $\lambda_{\text{ex}} = 505$ nm) was recorded. The fluorescence was fitted to the Stern-Volmer equation: $F_0/F = 1 + k[\text{Cl}]$, where F₀ is the fluorescence in the absence of chloride.

To measure the chloride permeability, the fluorescence was followed in liposomes after the addition of 50 mM KCl. After 10 min, 1 μM TBT

and 1 μM nigericin were added. The chloride concentration was calculated using the Stern-Volmer equation with k calculated from the titration curve.

Octanol Partitioning of Tamoxifen—The concentration of tamoxifen was measured by its absorbance peak at 245 nm. The A_{245} of 20 μM tamoxifen in phosphate-buffered saline, HCl, pH 1, or KOH, pH 13, solution was acquired. Then, 1 μl of octanol was added, the solution was vortexed, and the A_{245} of the aqueous phase was acquired.

RESULTS

In Vitro Acidification of Vesicles from Mammalian Cells

Total Microsomal Preparation—The mechanism by which tamoxifen inhibited acidification of intracellular organelles was first addressed by testing whether tamoxifen acted directly on the organelles or indirectly through soluble modulators. Acidification of organelles was assayed *in vitro* using microsomes isolated from MCF-7/ADR cells that are free of detectable soluble cytosolic proteins.

Acridine orange (AO) was used as a probe for luminal acidification (23). As vesicles acidify, they accumulate AO to self-quenching concentrations and deplete the extravesicular free AO, resulting in a decrease in total fluorescence. Acidification was initiated by the addition of ATP to a purified microsomal fraction in the absence of cytosol (Fig. 1A, at $t = 300$ s). Over the subsequent 1200 s, there was a reduction of the AO fluorescence, suggesting an accumulation of AO within the lumen of the microsomes. Nigericin, a K^+/H^+ exchanger that rapidly dissipates pH gradients, was added at the end of each reaction ($t = 1500$ s). In all experiments the AO fluorescence returned to its pre-ATP levels. This indicates that the decreased fluorescence was the consequence of the generation of a pH gradient.

When MCF-7/ADR vesicles were pretreated with tamoxifen for 30 min, there was a dose-dependent inhibition of AO quenching (Fig. 1A). Inhibition was evident when using 1 μM tamoxifen, and acidification was totally blocked with 8 μM tamoxifen. To quantify the effects of tamoxifen on acidification, we plotted acidification (as assayed by quenching of AO fluorescence) as a function of tamoxifen concentration (Fig. 1A, inset). The ID_{50} for maximal quenching is approximately 3 μM , which is in the same range that tamoxifen inhibits acidification *in vivo* (18). As a positive control, we employed bafilomycin A_1 , a potent and specific inhibitor of the vATPase responsible for acidification of all intracellular compartments (27).

To determine the time course for the inhibition of acidification by tamoxifen, the drug was added 10 min after addition of ATP (Fig. 1B). Addition of tamoxifen rapidly reversed acidification and caused an almost complete dissipation of the pH gradient within 5 min. Addition of bafilomycin A_1 dissipated the pH gradient at a much slower rate, even when used at 100 nM, which is 10 times the concentration that blocked 95% of acidification (see Fig. 1A). Addition of nigericin (Fig. 1B) and monensin (data not shown) dissipated the pH gradient significantly faster than tamoxifen. Thus, the time course of alkalization by tamoxifen is distinguishable from both rapidly acting electroneutral protonophores and inhibitors of the vATPase.

The fact that the *in vitro* acidification assay used purified microsomes in the absence of cytosolic or nuclear components indicates that the effects of tamoxifen on pH should be independent of cytosolic factors, such as the estrogen receptor, and of both transcription and translation. In addition, tamoxifen had similar effects on *in vitro* acidification of microsomes isolated from liver and kidney tissue from mice (data not shown). Therefore, the effect of tamoxifen on organelle acidification appears to be a general phenomenon.

***In Vitro* Acidification of Recycling Endosomes**—To specifically examine the acidification of the endosomes *in vitro*, we assayed *in vitro* acidification using FITC-transferrin which is constrained by the transferrin receptor to the endocytic path-

way. MCF-7/ADR cells were incubated with FITC-transferrin before lysis and isolation of microsomes. Since this assay is not based on the redistribution of probes, it further serves as verification that AO quenching resulted from vesicular acidification. Upon addition of ATP, there was a decrease in the ratio of the FITC emission (Fig. 1C). This signal was judged to be the consequence of acidification since it was reversed upon the addition of nigericin. The addition of 2.5 μM tamoxifen partially reversed the acidification in these organelles. This was further reduced by raising the tamoxifen concentration an additional 2.5 μM . This indicates that the recycling endosomes were one of the compartments in this *in vitro* assay whose acidification was blocked by tamoxifen.

Mechanisms of Organelle Acidification

Acidification of intracellular organelles utilizes an electrogenic proton pump (the vATPase) and chloride channels (28, 29). The vATPase couples ATP hydrolysis to proton movement. The unidirectional movement of the proton generates an inside positive V_m which limits acidification. The chloride channels allow passive chloride influx into the organelles, dissipating the V_m . Tamoxifen could inhibit acidification by the following possible mechanisms: direct inhibition of the vATPase; indirect inhibition of the vATPase through modulation of the V_m (such as blocking a chloride conductance); inhibition of acidification by a weak base effect or dissipation of pH gradients as a protonophore. There exists evidence in support of each of these mechanisms.

Inhibition of the vATPase—Tamoxifen has been reported to inhibit acid secretion by avian osteoclasts through inhibition of the plasma membrane vATPase activity. This activity has been attributed to the antagonism by tamoxifen of the membrane-bound calmodulin-dependent cyclic nucleotide phosphodiesterase, which regulates the vATPase (30).

Inhibition of the Chloride Channel—Tamoxifen has been reported to inhibit the volume-activated chloride channel (11).

Dissipation of pH Gradient by a Weak Base Effect—A weak base (such as ammonium chloride) will rapidly cross the membrane in a neutral (*i.e.* NH_3) form and bind protons in the interior causing an alkaline shift. The charged form of these molecules will accumulate according to the Henderson-Hasselbach equilibrium. Tamoxifen is a weak base with a pK_a of 6.9 when measured by NMR in 10% Triton solution (31). At a free tamoxifen concentration of 8 μM , a pH 7.3–5.3 gradient will result in <200 μM luminal concentration. This is less than the buffering capacity of the organelles, and this should not significantly perturb luminal pH. Thus, we initially considered this mechanism unlikely.

Dissipation of pH Gradient by Increasing Proton Permeability—Tamoxifen partitions into lipids, increases membrane fluidity, and decreases lipid peroxidation (32). If the charged protonated form of tamoxifen were membrane-permeable, tamoxifen would act like a classic protonophore. This mechanism has been proposed for the ability of many amine local anesthetics to uncouple respiration (33, 34).

Each of these potential mechanisms has distinct consequences for ATPase activity and V_m of the acidic organelle (Table I). If tamoxifen inhibits the vATPase, it would decrease the ATPase activity. In addition, it should decrease V_m of the organelles since the proton pumping is generating the V_m . If tamoxifen inhibits the chloride channel, it would increase V_m , since the chloride channel serves to dissipate V_m . As a consequence of the increased V_m , the vATPase cannot pump protons, resulting in a decreased rate of ATP hydrolysis. If tamoxifen is a protonophore, it should decrease V_m by allowing protons to permeate and increase ATPase activity by decreasing the elec-

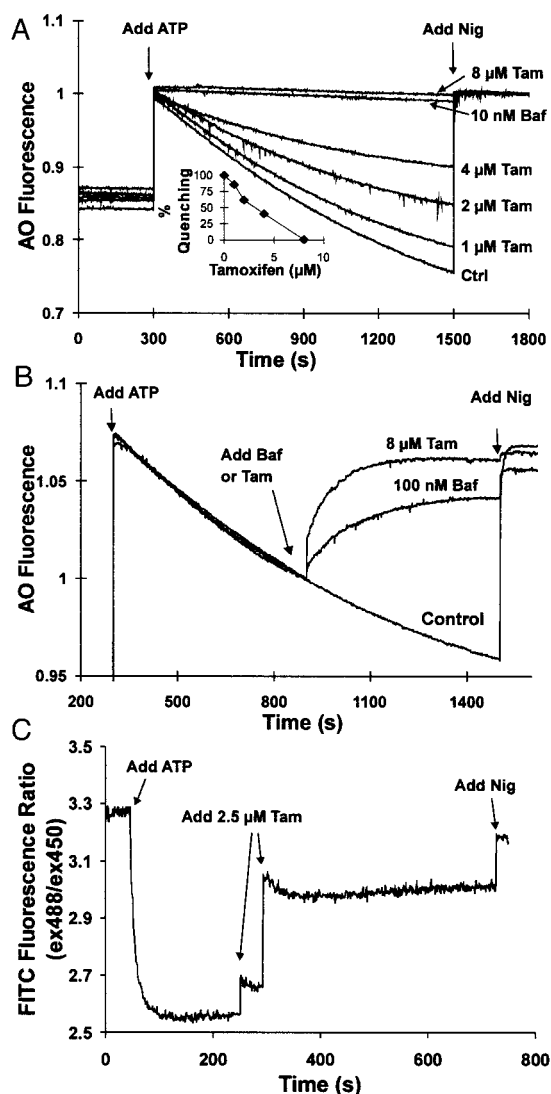


FIG. 1. Effect of tamoxifen on *in vitro* acidification of MCF-7/ADR organelles. *A*, preincubation with tamoxifen. Acridine orange is a weak base that accumulates to self-quenching concentrations into acidic compartments. Thus, the presence of acidic compartments decreases the total fluorescence by decreasing the concentration of free AO outside those compartments. Microsomes were suspended in AO, and after establishing base line, 1 mM Tris-ATP was added to begin acidification (at 300 s). This caused a slow decrease of total fluorescence over 1200 s (*Ctrl*). Addition of the protonophore nigericin (5 μM *Nig*) at $t = 1500$ returned the fluorescence levels demonstrating the fluorescence decrease was the consequence of acidification. This inhibitory effect of tamoxifen (*Tam*) on acidification was apparent at 1 μM and increased in a dose-dependent manner (2, 4, and 8 μM). Pretreatment of microsomes with 10 nM bafilomycin A₁ (*Baf*) also blocked acidification. *Inset*, dose-response of tamoxifen on acidification. Acidification was assayed as in *A*. *B*, tamoxifen added during the acidification. Ten minutes after the addition of 1 mM Tris-ATP, 8 μM tamoxifen or 100 nM bafilomycin A₁ was added which rapidly reversed acidification of the organelles. In the absence of tamoxifen or bafilomycin A₁, the organelles continued to acidify. Ten minutes later 5 μM nigericin was added. *C*, acidification in recycling endosomes assayed by FITC-transferrin. Cells were incubated with FITC-transferrin, which is endocytosed and localized within the endosomes. After lysing the cells a microsomal fraction was harvested. The fluorescence emission at 520 nm was monitored in response to excitation at 488 and 450 nm, and the ratio was plotted. When excited at 488 nm, the fluorescence of FITC increases with increasing pH, but when excited at 450 nm, the fluorescence of FITC is pH-independent. Therefore, a decreasing ratio indicates acidification. Upon addition of ATP ($t = 1080$ s) there was acidification of the lumen of the microsomes as assayed by a decrease in the ratio of the 488:450 nm emission. Nigericin was added ($t = 2500$ s) to confirm that the fluorescent shift was the result of acidification. Successive additions of 2.5 μM tamoxifen caused alkalization of endosomes. Nigericin was added at the end to equilibrate pH.

TABLE I
Predicted effects of potential mechanisms of tamoxifen on V_m and ATPase activity

	V_m	ATPase activity
Inhibit H-ATPase	Decrease	Decrease
Block counter-ion transport	Increase	Decrease
Increase proton permeability	Decrease	Increase
Weak base effect	Same to slight increase	Slight increase

trochemical gradient against which the vATPase must pump. A weak base should slightly increase V_m and ATPase activity since it dissipates the proton gradient in favor of an electrical gradient.

The predictions of these mechanisms were tested on isolated vacuoles from *S. cerevisiae*. Vacuoles from *S. cerevisiae* offer several advantages in biochemical studies of the actions of tamoxifen as follows. 1) They further address the specificity of the effects of tamoxifen (*S. cerevisiae* are known not to have an estrogen receptor). 2) They use the same basic machinery as mammalian organelles, a vATPase and chloride channel, to generate the proton gradient. 3) They can be purified in large amounts. It is very difficult to prepare mammalian organelles to the high purity required to assay V_m and ATPase activity. In yeast vacuole preparations, the vATPase represents ~50% of all ATPase activity, which is much higher than attainable for endosome or Golgi preparations.

In Vitro Acidification of Yeast Vacuoles and *E. coli* Membrane Vesicles

Acidification of Yeast Vacuoles—To test if tamoxifen inhibited acidification in yeast vacuoles, *in vitro* acidification of vacuoles was assayed using AO. The buffer was pre-equilibrated with either carrier (Me_2SO), tamoxifen (2 μM or 8 μM), ammonium chloride (1 mM), or concanamycin A (10 nM), or in potassium glutamate instead of KCl buffer (Fig. 2A). ATP (1.5 mM) was added at 50 s to initiate acidification, and at 400 s nigericin (1 μM) was added to dissipate pH gradients. As observed in mammalian microsomes, tamoxifen shows a dose-dependent inhibition of acidification, with complete inhibition at 8 μM. This strongly implies that tamoxifen inhibits acidification independent of the estrogen receptor which is not found in yeast. Acidification was slightly inhibited by the weak base ammonium chloride (1 mM). This is 1000-fold greater than the concentration of tamoxifen required to achieve similar inhibition.

Addition of tamoxifen to pre-acidified vacuoles (at 250 s in Fig. 2B) resulted in a rapid alkaline step followed by slower alkalization. The step is reminiscent of a weak base which rapidly establishes equilibrium across vesicles. Thus, a comparison was made of the effects of adding tamoxifen and the weak base ammonium to pre-acidified vacuoles (Fig. 2B). Addition of ammonium (1 mM) indeed caused a step alkalization. However, the vacuoles slowly re-acidify after addition of ammonium but continue to alkalize after addition of tamoxifen.

Membrane Potential—The fluorescent dye Oxonol V was used to monitor V_m . Oxonol V contains two delocalized negative charges and is highly lipophilic. In the presence of vesicles with positive V_m , it accumulates in the lumen and inner leaflet, resulting in fluorescence quenching (35). Unlike AO, which exhibits quenched fluorescence in the presence of acidified vesicles regardless of the number of non-acidified vesicles present, Oxonol V will report an average V_m for all vesicles. This necessitates the use of pure preparations, such as the yeast vacuoles.

The V_m was monitored in either KCl or potassium gluconate buffer (Fig. 3A). At 50 s, tamoxifen (10 μM) or carrier was added, and acidification was initiated by adding ATP (2.5 mM) at 200 s. A larger positive V_m was generated in potassium

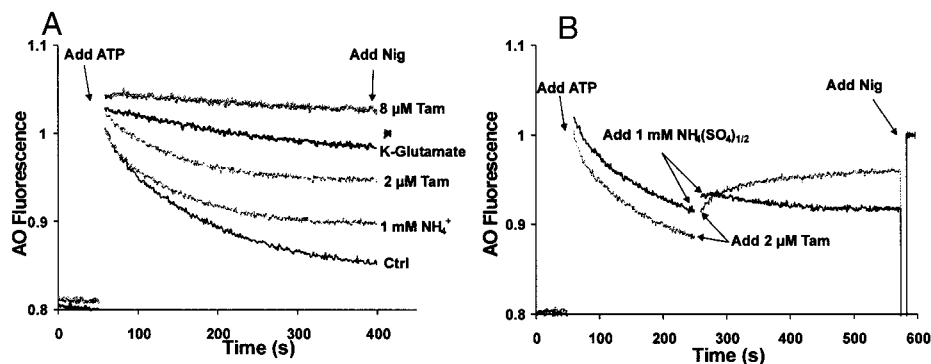


FIG. 2. Effect of tamoxifen on acidification of yeast vacuoles. *A*, effect of tamoxifen, ammonium sulfate, and chloride on yeast vacuole acidification. Vacuoles were suspended in buffer (KCl except potassium glutamate labeled) containing AO in the presence of tamoxifen (2 or 8 μM Tam), ammonium sulfate (1 mM NH_4^+), or potassium glutamate instead of KCl. ATP (1.5 mM) was added at 50 s to initiate acidification and nigericin (1 μM Nig) was added at 400 s. The presence of tamoxifen caused a dose-dependent inhibition of acidification. Ammonium sulfate, at much higher concentrations, also caused a slight inhibition. When glutamate was used instead of chloride, acidification decreased, consistent with a chloride channel dissipating the V_m . *B*, effect of adding tamoxifen or ammonium sulfate during acidification of yeast vacuoles. Vacuoles were in a KCl buffer containing AO, and acidification was initiated by addition of ATP (1.5 mM) at 50 s. At 250 s, either ammonium sulfate (1 mM) or tamoxifen (2 μM) was added. Each caused a step increase in AO fluorescence, indicating alkalization. Subsequently, AO fluorescence continued to increase when tamoxifen was added but slowly decreased when ammonium sulfate was added.

gluconate than in KCl which implicates a chloride permeability in dissipating the V_m of the vacuoles. Tamoxifen significantly decreased the V_m generated by the vATPase. This suggests that tamoxifen may increase ion permeability thus decreasing the V_m .

ATPase Activity—To assay specifically the vATPase activity, the effects of tamoxifen were quantified on the bafilomycin-inhibitable ATPase activity. Replacing chloride with gluconate decreased the bafilomycin-inhibitable ATPase activity (Fig. 3B), further confirming that chloride provided the counter-ion transport to dissipate the V_m . Addition of tamoxifen caused an increase of ATPase activity in both conditions, with a more dramatic increase in gluconate buffer (Fig. 3B).

In summary, in yeast vacuoles tamoxifen inhibited ATP-dependent acidification, decreased V_m , and increased bafilomycin-inhibitable ATPase activity. These observations are consistent with the hypothesis that tamoxifen increases membrane permeability to protons, either through direct lipid interaction or through proteins or modulators (Table I).

Acidification of *E. coli* Inverted Membrane Vesicles—To test the protein and lipid specificity of acidification inhibition by tamoxifen, the effects of tamoxifen on ATP-dependent acidification in *E. coli* inverted vesicles (InV) was assayed. Unlike mammalian or yeast vesicles, InV utilize the F_0F_1 -ATPase for acidification and are composed of different types of lipids, including an abundance of cardiolipin and a lack of sterols.

As shown in Fig. 4, the presence of tamoxifen inhibited acidification in InV with a similar dose dependence as observed in mammalian and yeast vesicles (Figs. 1A and 2A). Similarly, addition of tamoxifen to *E. coli* vesicles pre-acidified with ATP resulted in similar rates of alkalization (data not shown) as mammalian and yeast vesicles (Figs. 1A and 2A). These observations indicate that tamoxifen can dissipate pH gradients across a diverse spectrum of native biological membranes.

Liposomes

pH Gradients—The effect of tamoxifen on pH gradients was tested in pure lipid vesicles. This system was used both because the effects of tamoxifen on acidification were observed in diverse biological membranes and because the results on the ATPase activity were consistent with tamoxifen affecting membrane permeability to protons.

Liposomes were loaded with pyranine, a hydrophilic, non-permeable fluorescent pH indicator to assay proton permeability. The log of the ratio of the fluorescence emission of pyranine

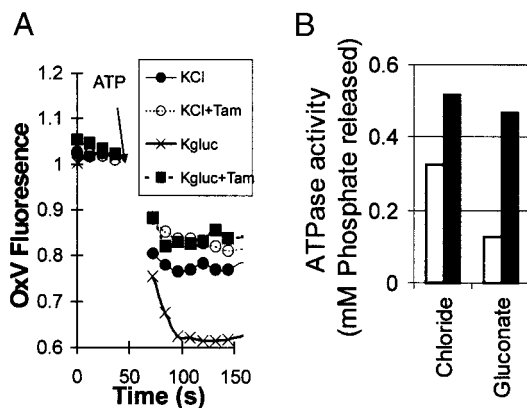


FIG. 3. Effect of tamoxifen on V_m and vacuolar ATPase activity of yeast vacuoles. *A*, effect of tamoxifen (Tam) and chloride on V_m of yeast vacuoles. Vacuoles were suspended in KCl or potassium gluconate (Kgluc) buffer with 1 μM Oxonol V (OxV). Oxonol V is a membrane-permeable anionic dye. Thus, it accumulates into vesicles of positive V_m , resulting in fluorescence quenching. Addition of ATP resulted in a vATPase generated inside-positive V_m of the vacuoles and quenching of Oxonol V fluorescence. In the absence of tamoxifen, the V_m was greater in potassium gluconate than KCl, consistent with a chloride channel dissipating the V_m . The presence of tamoxifen decreased the ATP-generated V_m in both KCl and potassium gluconate to similar levels. *B*, effect of tamoxifen and chloride on bafilomycin-inhibitable ATPase activity of yeast vacuoles. ATPase levels were quantified by measuring released phosphate as described under "Experimental Procedures." Samples were split in two and processed \pm bafilomycin A1 to determine vATPase activity. In the absence of tamoxifen, ATPase activity was greater in chloride than gluconate. This is because in the absence of chloride, there is a large V_m against the vATPase. Tamoxifen increased the ATPase activity in both buffers.

when excited at $\lambda_{\text{ex}} = 405$ nm and $\lambda_{\text{ex}} = 455$ nm is linearly dependent on the pH (Fig. 5) (36, 37). Two steps were taken to ensure that only pH_L was measured and to permit the discrimination between dissipation of pH gradient and the lysis or dye leakage from liposomes. First, greater than 95% of external pyranine was removed by gel filtration. Second, the membrane-impermeable quencher DPX was added to the external solution (38) which effectively quenched all remaining non-luminal pyranine fluorescence.

To mimic the acidified lumen of organelles, liposomes were made with the pH_L buffered at 6.2. The pH_L was monitored while the external pH (at 50 s) was shifted to 7.3 (Fig. 6A) in

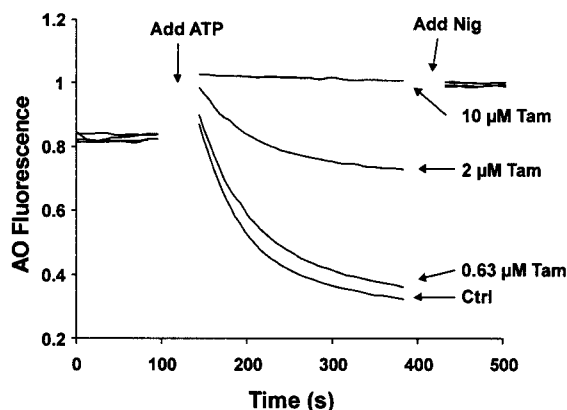


FIG. 4. Effect of tamoxifen on acidification of *E. coli* inverted membrane vesicles. InV were suspended in KCl buffer with $6 \mu\text{M}$ AO in the presence (0.63 , 2 , and $10 \mu\text{M}$) or absence of tamoxifen (*Tam*). ATP (1.5 mM) and nigericin (*Nig*) ($1 \mu\text{M}$) were added at 100 and 400 s . Similar to both mammalian microsomes (Figs. 1 and 2) and yeast vacuoles (Fig. 3), tamoxifen inhibited ATP-dependent acidification.

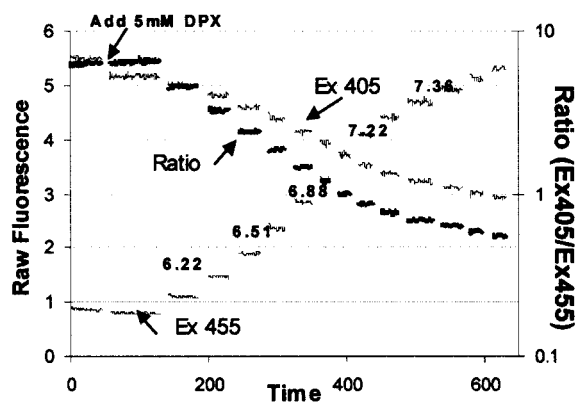


FIG. 5. Titration curve of pyranine-loaded liposomes. Pyranine is a non-membrane-permeable ratiometric pH indicator. Its acidic form is fluorescent when excited at 405 nm , and its basic form is fluorescent when excited at 455 nm . Liposomes ($\text{pH}_{\text{in}} 6.3$) were loaded with pyranine and diluted into buffer with $\text{pH}_{\text{out}} 6.3$ in the presence of nigericin, to allow rapid equilibration between internal and external pH. The raw fluorescence when excited at 405 and 455 (left axis) as well as the ratio (right axis, log scale) were monitored. DPX, a non-permeable quencher of pyranine fluorescence, was added and decreased the raw fluorescence by only the dilution factor, indicating that virtually all pyranine fluorescence is from the liposome lumen. Aliquots of MES were added to decrease the external pH and internal pH (due to the presence of nigericin), and the pH was measured using a pH meter. There was no decrease in total fluorescence throughout the experiment, indicating no dye leakage or DPX influx.

the presence tamoxifen (0 , 0.5 , or $2 \mu\text{M}$). Nigericin ($1 \mu\text{M}$) was added at 700 s to dissipate pH gradients. In the absence of tamoxifen, the pH_{L} increased less than 0.2 pH units over the 10-min span. In the presence of tamoxifen, after a shift of external pH, there was a rapid step increase in pH_{L} . The proton permeability of liposomes after the step increase is difficult to compare with the control, since the pH gradient has decreased. Tamoxifen did not induce detectable leakage of pyranine, and in solution, tamoxifen does not affect pyranine fluorescence (data not shown).

The effects of tamoxifen on pH_{L} were contrasted with the effects of other pH perturbants with known mechanisms of action, specifically a protonophore (FCCP), a potassium ionophore (valinomycin), and a weak base (NH_4Cl) (Fig. 6B). FCCP at saturating concentrations only slowly dissipated the pH gradient. This is because FCCP allows free movement of only protons. Thus proton efflux down its gradient generates a V_m preventing further proton movement. The presence of valino-

mycin, a K^+ -selective ionophore which would dissipate V_m , caused a faster dissipation of the pH gradient than FCCP (Fig. 6C). Here, protons can efflux down the concentration gradient without generation of V_m . Thus, these liposomes were more permeable to protons than potassium. As expected, the combination of FCCP and valinomycin immediately dissipated the pH gradient (data not shown) comparable with the effects of nigericin. The weak base NH_4Cl caused a step alkaline shift, followed by a slow alkaline drift. Here, the alkaline shift is caused by the selective diffusion of the basic NH_3 into the vesicles, whereas the acidic NH_4^+ is impermeable. Of the three agents tested, the effect of micromolar concentrations of tamoxifen is most similar to the effect observed at millimolar concentrations of NH_4Cl ; the step alkalization upon changing the external pH was similar, but the subsequent dissipation of pH was faster with $0.5 \mu\text{M}$ tamoxifen (Fig. 6A).

The potential contribution of a weak base effect in the mechanism of tamoxifen action was further explored using liposomes in the absence of a pre-existing pH gradient. The pH_{L} was monitored and tamoxifen (2 and $8 \mu\text{M}$) or NH_4Cl (5 mM) was added at 50 s . At 700 s , nigericin was added to dissipate the pH gradient. As expected, upon addition of the weak base NH_4Cl , the non-protonated species (NH_3) rapidly diffused into the liposomes, where it was protonated causing alkalization of the lumen (Fig. 7A). The pH gradient slowly dissipated by either leakage of H^+ or NH_4^+ . Similarly, addition of tamoxifen caused alkalization of liposomes, followed by more rapid pH equilibration (Fig. 7A). This suggests that like ammonia, tamoxifen-free base rapidly enters liposomes, causing a step alkaline shift in the lumen while the protonated tamoxifen is less permeable.

The observation that tamoxifen exerted similar effects to NH_4Cl at 3 orders of magnitude lower concentration suggests that it may be highly concentrated within liposomes. The extent of lipid partitioning of tamoxifen was examined by measuring the partitioning coefficient of tamoxifen between octanol and aqueous buffer. Tamoxifen in aqueous solution was equilibrated with either $1:1000$ or $1:100$ volume of octanol, and the concentration of tamoxifen left in the aqueous phase was measured by absorbance (Fig. 7B). Notice that $1:1000$ volume octanol was able to extract approximately 50% of tamoxifen in aqueous solution, suggesting that tamoxifen partitions 3 orders of magnitude greater into the lipid phase. Octanol partitioning was repeated with the aqueous phase buffered to $\text{pH} 1$ and $\text{pH} 13$ to examine possible differences in partitioning between the charged and neutral forms of tamoxifen, respectively. The same result was obtained at both pH values (data not shown). This is consistent with the difference in concentrations of NH_4Cl and tamoxifen required for the same quantitative effect. It may also contribute to the observation that pyranine reports a lower pH_{L} in the presence of tamoxifen even after addition of nigericin (Fig. 7A). Tamoxifen could effectively give the liposomes a positive surface charge, which has been shown to effect pyranine fluorescence (36).

In both yeast vacuoles (Fig. 2B) and liposomes (Fig. 7A), addition of tamoxifen or ammonium caused similar pH jumps, but tamoxifen subsequently caused a more rapid equilibration of pH. This suggests that other mechanism(s) may contribute in addition to the weak base effect. In liposomes with an acidic lumen, the initial weak base alkaline jump is too large to allow an assessment of the rate of subsequent pH dissipation. Therefore, we tested the effects of tamoxifen and a weak base on liposomes with an alkaline interior pH of 8.1 . The pH_{L} was monitored after shifting the external pH to 6.9 by the addition of 4 mM MES, $\text{pH} 5$, at 50 s (Fig. 8A). The pH gradient was dissipated more quickly with increasing concentrations of ta-

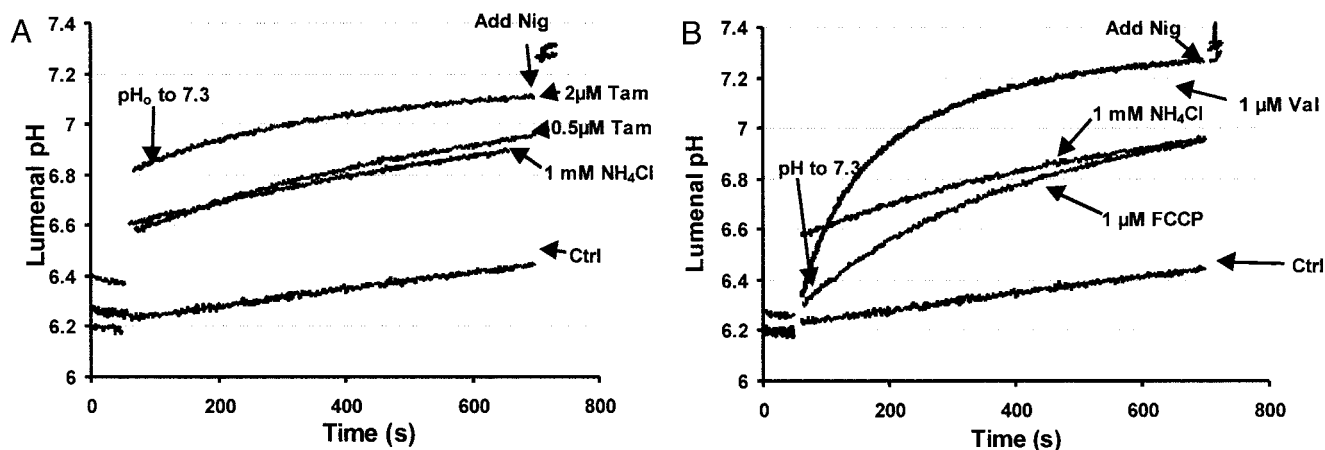


FIG. 6. **Rate of pH equilibration of pH 6.3 liposomes in a pH 7.3 bath.** Pyranine-loaded liposomes with pH_{in} 6.3 was diluted into KCl buffer of same pH and 10 mM DPX and one of the following compounds: carrier, tamoxifen (*Tam*) (0.5 and 2 μ M), NH_4Cl (1 mM), FCCP (1 μ M), or valinomycin (*Val*) (1 μ M). At 20 s, 5 mM potassium glycyglycine, pH 8.4, was added to raise pH_{out} to 7.3. At 700 s, 1 μ M nigericin (*Nig*) was added to equilibrate pH. *A*, with the presence of tamoxifen, the pH shift caused a rapid alkaline shift of the lumen. This cannot be due to lysis because there was no decrease of total fluorescence indicating lack of dye leakage into DPX-containing external buffer. Ammonium, at 2000 \times concentration, caused a similar alkaline jump. But the rate of pH dissipation was faster after the alkaline jump with tamoxifen than ammonium. *B*, FCCP and valinomycin each increased the rate of pH dissipation, but did not cause an alkaline jump upon change of external pH.

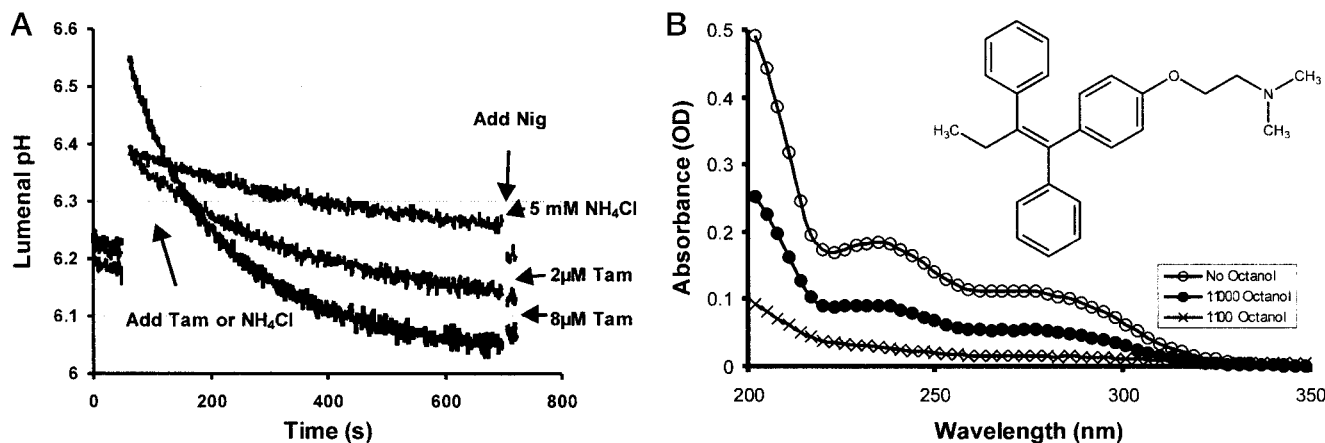


FIG. 7. **Basis for weak base effect of tamoxifen.** *A*, effect on liposome pH by weak base addition. Pyranine-loaded liposomes with pH_{in} 6.3 were diluted into KCl buffer of same pH and 10 mM DPX. At 50 s, tamoxifen (*Tam*) (2 and 8 μ M) or NH_4Cl (5 mM) was added. At 700 s, nigericin (*Nig*) (1 μ M) was added. Addition of tamoxifen or NH_4Cl resulted in alkalization of the lumen, presumably due to selective influx and protonation of the uncharged species. Importantly, following the alkaline jump, the pH re-equilibrated much faster when tamoxifen was used, suggesting a tamoxifen-mediated proton permeability. *B*, octanol partitioning of tamoxifen. Tamoxifen (20 μ M) in phosphate-buffered saline was mixed with 1:1000 or 1:100 volume of octanol. The tamoxifen concentration of the aqueous phase was determined using absorbance spectroscopy. Notice the 1:1000 volume octanol was able to extract approximately ~50% tamoxifen from the aqueous phase. This suggests that tamoxifen partitions 3 orders of magnitude into the lipid phase and is consistent with the potency of tamoxifen compared with ammonium in *A*.

moxifen. In contrast, the effect of NH_4Cl (10 mM) was indistinguishable from the control. Thus, the dissipation of pH by tamoxifen cannot be solely explained as a weak base effect.

To explore potential ionophoretic mechanisms, tamoxifen was compared with FCCP and valinomycin (Fig. 8*B*). Addition of FCCP did not substantially increase the rate by which the pH gradient was dissipated, presumably because proton leakage is limited by the V_m . This is substantiated by the observation that valinomycin caused a greater dissipation of the pH gradient than FCCP.

The observation that tamoxifen diminished the pH gradient faster than a saturating concentration of FCCP (Fig. 8*B*) implies that tamoxifen cannot be a pure protonophore. Any pure protonophore will, like FCCP, allow free proton movement but be limited by V_m . Importantly, when both tamoxifen and valinomycin were included, the effect was *additive* and not synergistic. This implies that tamoxifen mediated proton movement is *electroneutral*. If tamoxifen mediated an electrogenic process (e.g. pure protonophore), the dissipation of the V_m by valinomycin would dramatically increase the effect of tamoxifen. For

example, the presence of valinomycin allows FCCP to immediately dissipate any pH gradient.

Chloride Permeability—If tamoxifen mediates bi-directional electroneutral transport of protons, then a second ion must be co-transported. We first asked if this ion could be chloride. We examined the effect of tamoxifen on the influx of chloride into liposomes. Lucigenin, a fluorescent dye that is collisionally quenched by chloride, was employed (39). Liposomes were loaded with KNO_3 buffer and lucigenin. The luminal chloride concentration can be accurately calibrated by the fluorescence (data not shown).

Luminal chloride concentration in the liposomes was monitored after addition of 50 mM KCl to the external solution (Fig. 9*A*). Tamoxifen caused a dose-dependent increase in the rate of chloride influx. Since chloride is more membrane-permeable than potassium, unidirectional chloride movement is also expected to be limited by V_m (40). Indeed, the presence of valinomycin increased the rate of chloride equilibration. To test if tamoxifen was affecting chloride permeability solely by dissipation of the V_m , tamoxifen was added to liposomes in the

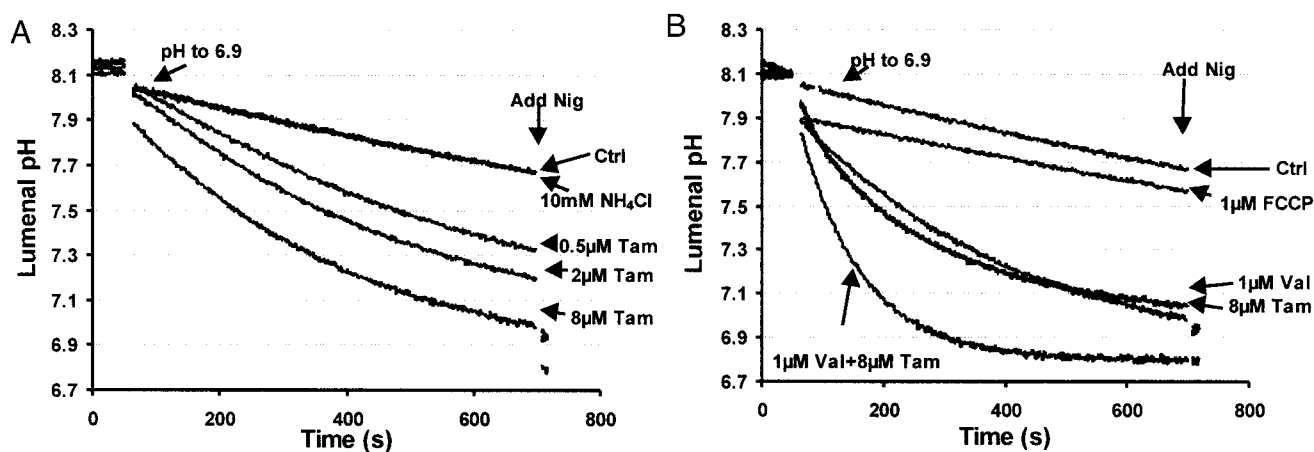


FIG. 8. Rate of pH equilibration of pH 8.1 liposomes in a pH 6.9 bath. Pyranine-loaded liposomes with pH_{in} 8.1 was diluted into KCl buffer of the same pH and 10 mM DPX and one of the following compounds: carrier, tamoxifen (*Tam*) (0.5, 2, and 8 μ M), NH_4Cl (10 mM), FCCP (1 μ M), valinomycin (*Val*) (1 μ M), or both tamoxifen (8 μ M) and valinomycin (1 μ M). At 50 s, 5 mM K-MES was added to lower pH_{out} to 6.9. A, increasing concentrations of tamoxifen caused a dose-dependent increase of pH equilibration. The weak base NH_4Cl , at 10 \times concentration used to observe a significant weak base effect (Fig. 6), had no effect. B, FCCP and valinomycin each increased the rate of pH dissipation. Tamoxifen increased the rate faster than saturating concentrations of FCCP. Tamoxifen and valinomycin together were additive and not synergistic. These two observations suggest that tamoxifen cannot be a pure protonophore but must mediate an electroneutral process. *Nig*, nigericin.

presence of a concentration of valinomycin (1 μ M) that completely dissipates the V_m (Fig. 9A). The addition of 4 μ M tamoxifen increased the rate of chloride influx observed in the presence of valinomycin. This suggests that tamoxifen must be having an effect on chloride permeability independent of any effects on V_m . In addition, the fact that the effects tamoxifen and valinomycin were additive on chloride permeability also suggests that the chloride transport is electroneutral.

Since tamoxifen seems to increase both proton and chloride permeability, we next addressed the question of whether tamoxifen mediates their coupled transport (*i.e.* the crossing of HCl but not H^+ or Cl^- independently). If tamoxifen mediates coupled transport, then chloride would be necessary for tamoxifen-mediated proton permeability. Thus, we assessed the effect of tamoxifen on pH in the absence of chloride. Pyranine-loaded liposomes with a luminal pH of 8.1 were resuspended in 300 mM potassium glutamate and then the external pH was shifted to 6.9 (Fig. 9B). Tamoxifen had no effect on the dissipation of pH. Inclusion of 90 mM KCl resulted in more rapid pH equilibration (Fig. 9B). In the absence of tamoxifen, addition of 90 mM KCl had no effect (data not shown). This indicates that external chloride is required for tamoxifen-mediated acidification of the lumen of the liposomes.

To further test if tamoxifen is acting as a coupled Cl^-/H^+ co-transporter, we analyzed the effect of chloride gradients on luminal pH in the presence of tamoxifen. In liposomes with no luminal chloride, addition of KCl to the external solution results in a large chloride gradient. If tamoxifen were acting as a coupled Cl^-/H^+ co-transporter, the chloride influx should mediate proton influx and luminal acidification. Liposomes were equilibrated to pH 8.0 both inside and out (Fig. 9C). Upon addition of tamoxifen there was a rapid step alkaline shift of the lumen of the liposomes due to a weak base effect. Moreover, upon each successive addition of 50 mM KCl there was an acidic shift of the luminal pH. This suggests that tamoxifen-coupled HCl transport mediates the rapid re-equilibration and explains why re-equilibration is faster when tamoxifen was added compared with NH_4Cl .

DISCUSSION

Tamoxifen inhibits ATP-dependent acidification in intact cells (18), mammalian organelles (Fig. 1), yeast vacuoles (Fig. 2), and InV (Fig. 4). It also dissipates pH gradients in liposomes

(Figs. 6–9). The tamoxifen-dependent dissipation of the pH gradient is independent of all proteins including the estrogen receptor.

Our results suggest that tamoxifen affects transmembrane pH through at least two independent mechanisms as follows: as a weak base and as a mediator of coupled transport of proton/hydroxide and chloride. For vesicles with an acidified lumen, tamoxifen causes a rapid alkaline shift of the pH_L which is most likely a weak base effect (Fig. 10). We propose tamoxifen is highly concentrated within the leaflets of membranes. Since tamoxifen is a weak base, its neutral form can readily flip between inner and outer leaflets while the charged form flips much less readily. Therefore, it will accumulate within the inner leaflet of acidic organelles, causing a step alkalization.

However, a weak base effect is not sufficient to account for many of the effects of tamoxifen on transmembrane pH. Tamoxifen, but not ammonium, can increase pH equilibration rate when the lumen of the liposome is alkaline relative to the bath. Furthermore, chloride is necessary for tamoxifen-mediated proton permeability, and a chloride gradient can generate a pH gradient in the presence of tamoxifen. One possible mechanism for this process is that the permeability of the protonated form of tamoxifen increases when it is conjugated to chloride (Fig. 10).

The fact that tamoxifen inhibits acidification in so many model systems indicates that tamoxifen should affect organellar pH in many different cell types. This is consistent with the observations that tamoxifen administration has numerous physiological sequelae that are not restricted to cells expressing the estrogen receptor. Of particular significance is the observation that blocking organelle acidification through other means is sufficient to reproduce many of the effects of tamoxifen. Tamoxifen blocks bone resorption which is also blocked by antagonists of the vATPase (19). In drug-resistant tumor cells tamoxifen redistributes chemotherapeutics from the organelles to the cytoplasm (18) and increases the sensitivity of the cells to chemotherapeutics (41). These effects can be reproduced solely by mimicking the effects of tamoxifen on organellar acidification either with the use of protonophores, weak bases, or inhibitors of the vATPase (9, 22, 41). Tamoxifen decreases the rate of vesicle sorting and secretion (18) which is also seen when organelle acidification is blocked with protonophores

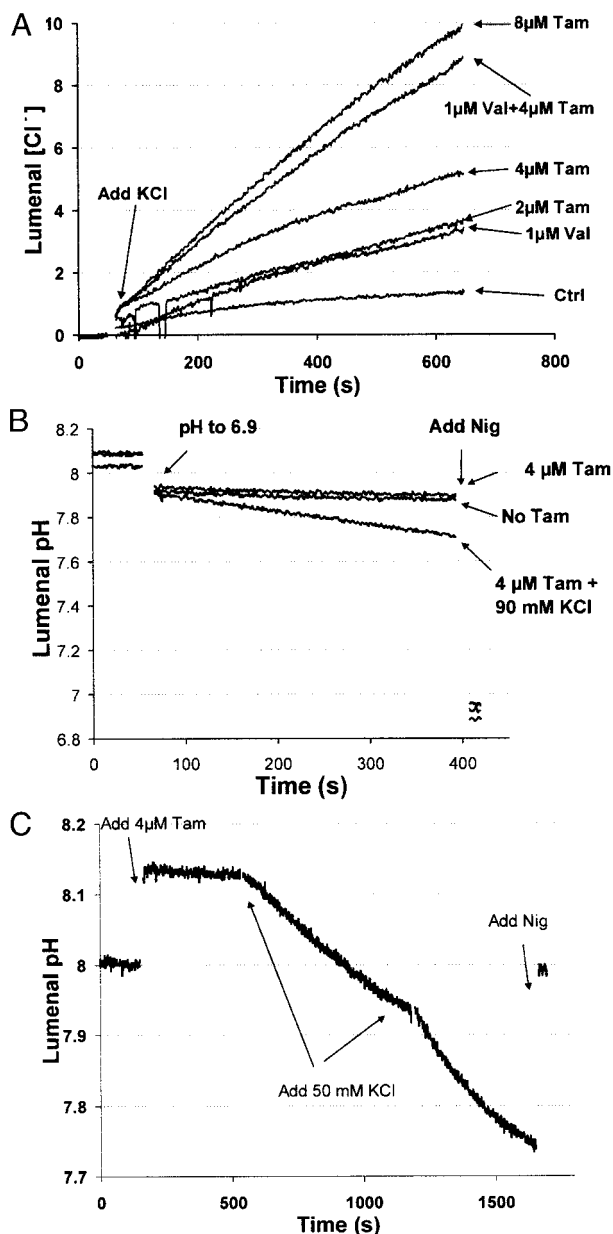


FIG. 9. Effect of chloride on tamoxifen-mediated proton permeability. *A*, rate of chloride influx into liposomes. Lucigenin, a non-permeable fluorescent probe that is collisionally quenched by chloride, was used to assay liposome chloride concentration. Lucigenin-loaded liposomes made with an internal solution of 150 mM KNO₃ were diluted into 150 mM KNO₃ buffer and one of the following compounds: carrier, tamoxifen (*Tam*) (2, 4, and 8 μM), valinomycin (*Val*) (1 μM), or both tamoxifen (4 μM) and valinomycin (1 μM). At 50 s, 50 mM KCl was added, and the internal chloride concentration was followed using lucigenin fluorescence. Tamoxifen caused a dose-dependent chloride influx. Valinomycin also increased chloride influx by dissipating V_m . Importantly, tamoxifen and valinomycin together were additive, implying that tamoxifen is not a pure chloride ionophore but mediates electroneutral chloride influx. *B*, effect of chloride on tamoxifen-mediated proton permeability. Pyranine-loaded liposomes made with internal solution of 300 mM potassium glutamate, pH 8.1, was diluted into the same external solution in the presence or absence of tamoxifen and 50 mM KCl as denoted in legend. At 50 s, pH_{out} was shifted to pH 6.9 and pH_{in} was followed. In the absence of chloride, tamoxifen had no effect on the rate of pH equilibration. The presence of chloride reconstituted the effect of tamoxifen seen in Fig. 8. *C*, liposomes made as in *B* were diluted into 300 mM potassium glutamate solution. Addition of 4 μM tamoxifen caused an alkaline shift similar to Fig. 7A. But the rate of re-equilibration was much slower than in Fig. 7A. Addition of 2 aliquots of 50 mM KCl caused increasing rate of acidification, presumably due to Cl⁻/H⁺ co-influx. *Nig*, nigericin.

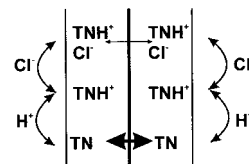


FIG. 10. Model for tamoxifen-mediated proton permeability. Tamoxifen is concentrated within the lipid bilayer and exists as a charged protonated form (TNH⁺) or uncharged form (TN). The uncharged form is readily membrane-permeable, and the charged form is impermeable. This accounts for the weak base activity of tamoxifen. In addition, TNH⁺ can permeate the membrane when carrying a chloride ion, accounting for the chloride-dependent electroneutral proton permeability.

(42). Many secreted proteins are activated by a pH-dependent proteolytic step in the Golgi. Thus, the reduced activity of many secreted proteins observed with tamoxifen treatment may also be the consequence of a tamoxifen block of organelle acidification.

Consistent with previous reports (43), we observe that tamoxifen accumulates in the lipid phase (1000:1) over the aqueous environment. Furthermore, our results suggest that membrane-bound tamoxifen is in equilibrium between a neutral and protonated form. Thus, tamoxifen would be expected to significantly perturb many properties of cellular membranes, including increased surface charge, and altered membrane tension. These effects have been reported for lipophilic weak base anesthetics (44–46). The altered membrane properties could shift the voltage dependence of many ion channels. Indeed, tamoxifen has been reported to shift the activity of many ion channels (11–16). Detailed studies on the model channel, gramicidin, have shown that membrane tension (47) and surface charge (48) are critical determinants of channel activity.

These results demonstrate that many of the effects of tamoxifen on cells can be attributed to either membrane-active effects on organelle acidification or surface charge. Each of these effects are independent of the estrogen receptor. This suggests that it should be possible to screen for other estrogen-receptor antagonists that do not also affect organelle acidification and therefore may not share the same physiological effects as tamoxifen.

Acknowledgments—We thank Nihal Altan, Jamie M. Hahn, Judith A. Hirsch, Elliott M. Kanner, and Denise K. Marciano for valuable comments and discussion.

REFERENCES

- Jaiyesimi, I. A., Buzdar, A. U., Decker, D. A., and Hortobagyi, G. N. (1995) *J. Clin. Oncol.* **13**, 513–529
- Jordan, V. C. (1995) *Proc. Soc. Exp. Biol. Med.* **208**, 144–149
- Fisher, B., Costantino, J. P., Wickerham, D. L., Redmond, C. K., Kavanah, M., Cronin, W. M., Vogel, V., Robidoux, A., Dimitrov, N., Atkins, J., Daly, M., Wieand, S., Tan-Chiu, E., Ford, L., and Wolmark, N. (1998) *J. Natl. Cancer Inst.* **90**, 1371–1388
- Kellen, J. A. (ed) (1996) *Tamoxifen: Beyond the Antiestrogen*, Birkhauser Boston, Inc., Cambridge, MA
- Chatterjee, M., and Harris, A. L. (1990) *Br. J. Cancer* **62**, 712–717
- Berman, E., Adams, M., Duigou-Osterndorf, R., Godfrey, L., and Clarkson, B. A. M. (1991) *Blood* **77**, 818–825
- Berman, E., McBride, M., Lin, S., Menedez-Botet, C., and Tong, W. (1995) *Leukemia (Balt.)* **9**, 1631–1637
- Weinlander, G., Kornek, G., Raderer, M., Hejna, M., Tetzner, C., and Scheithauer, W. (1997) *J. Cancer Res. Clin. Oncol.* **123**, 452–455
- Altan, N., Chen, Y., Schindler, M., and Simon, S. M. (1998) *J. Exp. Med.* **187**, 1583–1598
- Love, R. R., Mazess, R. B., Barden, H. S., Epstein, S., Newcomb, P. A., Jordan, V. C., Carbone, P. P., and DeMets, D. L. (1992) *N. Engl. J. Med.* **326**, 852–856
- Zhang, J. J., Jacob, T. J., Valverde, M. A., Hardy, S. P., Mintenig, G. M., Sepulveda, F. V. G. D., Hyde, S. C., Trezise, A. E., and Higgins, C. F. (1994) *J. Clin. Invest.* **94**, 1690–1697
- Ehring, G. R., Osipchuk, Y. V., and Cahalan, M. D. (1994) *J. Gen. Physiol.* **104**, 1129–1161
- Greenberg, D. A., Carpenter, C. L., and Messing, R. O. (1987) *Cancer Res.* **47**, 70–74
- Song, J., Standley, P. R., Zhang, F., Joshi, D., Gappy, S., Sowers, J. R., and

- Ram, J. L. (1996) *J. Pharmacol. Exp. Ther.* **277**, 1444–1453
15. Williams, J. P., Blair, H. C., McKenna, M. A., Jordan, S. E., and McDonald, J. M. (1996) *J. Biol. Chem.* **271**, 12488–12495
16. Turner, R. T., Wakley, G. K., Hannon, K. S., and Bell, N. H. (1988) *Endocrinology* **122**, 1146–1150
17. Callaghan, R., and Higgins, C. F. (1995) *Br. J. Cancer* **71**, 294–299
18. Altan, N., Chen, Y., Schindler, M., and Simon, S. M. (1999) *Proc. Natl. Acad. Sci. U. S. A.* **96**, 4432–4437
19. Sundquist, K., Lakkakorpi, P., Wallmark, B., and Vaananen, K. (1990) *Biochem. Biophys. Res. Commun.* **168**, 309–313
20. Gekle, M., Mildenberger, S., Freudinger, R., and Silbernagl, S. (1995) *Am. J. Physiol.* **268**, F899–F906
21. van Weert, A. W., Dunn, K. W., Gueze, H. J., Maxfield, F. R., and Stoorvogel, W. (1995) *J. Cell Biol.* **130**, 821–834
22. Hurwitz, S. J., Terashima, M., Mizunuma, N., and Slapak, C. A. (1997) *Blood* **89**, 3745–3754
23. Barasch, J., Kiss, B., Prince, A., Saiman, L., Gruenert, D., and Al-Awqati, Q. (1991) *Nature* **352**, 70–73
24. Roberts, C. J., Raymond, C. K., Yamashiro, C. T., and Stevens, T. H. (1991) *Methods Enzymol.* **194**, 644–661
25. Simon, S. M. and Blobel, G. (1992) *Cell* **69**, 677–684
26. Biversi, J., Tulk, B., and Verkman, A. S. (1994) *Anal. Biochem.* **219**, 139–143
27. Bowman, E. J., Siebers, A., and Altendorf, K. (1988) *Proc. Natl. Acad. Sci. U. S. A.* **85**, 7972–7976
28. Glickman, J., Croen, K., Kelly, S., and Al-Awqati, Q. (1983) *J. Cell Biol.* **97**, 1303–1308
29. Mellman, I., Fuchs, R., and Helenius, A. (1986) *Annu. Rev. Biochem.* **55**, 663–700
30. Williams, J. P., McDonald, J. M., McKenna, M. A., Jordan, S. E., Radding, W., and Blair, H. C. (1997) *J. Cell. Biochem.* **66**, 358–369
31. Bottega, R., and Epand, R. M. (1992) *Biochemistry* **31**, 9025–9030
32. Wiseman, H., Quinn, P., and Halliwell, B. (1993) *FEBS Lett.* **330**, 53–56
33. Garlid, K. D., and Nakashima, R. A. (1983) *J. Biol. Chem.* **258**, 7974–7980
34. Sun, X., and Garlid, K. D. (1992) *J. Biol. Chem.* **267**, 19147–19154
35. Scherman, D., and Henry, J. P. (1980) *Biochim. Biophys. Acta* **599**, 150–166
36. Kano, K., and Fendler, J. H. (1978) *Biochim. Biophys. Acta* **509**, 289–299
37. Clement, N. R., and Gould, J. M. (1981) *Biochemistry* **20**, 1534–1538
38. Ladokhin, A. S., Wimley, W. C., and White, S. H. (1995) *Biophys. J.* **69**, 1964–1971
39. Biversi, J., Emans, N., and Verkman, A. S. (1996) *Proc. Natl. Acad. Sci. U. S. A.* **93**, 12484–12489
40. Paula, S., Volkov, A. G., Van Hoek, A. N., Haines, T. H., and Deamer, D. W. (1996) *Biophys. J.* **70**, 339–348
41. Schindler, M., Grabski, S., Hoff, E., and Simon, S. M. (1996) *Biochemistry* **35**, 2811–2817
42. Tartakoff, A. M. (1983) *Cell* **32**, 1026–1028
43. Wiseman, H. (1994) *Trends Pharmacol. Sci.* **15**, 83–89
44. Gruner, S. M., and Shyamsunder, E. (1991) *Ann. N. Y. Acad. Sci.* **625**, 685–697
45. Seelig, A., Allegrini, P. R., and Seelig, J. (1988) *Biochim. Biophys. Acta* **939**, 267–276
46. Sato, K., Kojima, K., and Sato, C. (1977) *Tohoku J. Exp. Med.* **123**, 185–190
47. Goulian, M., Mesquita, O. N., Fygenson, D. K., Nielsen, C., Andersen, O. S., and Libchaber, A. (1998) *Biophys. J.* **74**, 328–337
48. Rostovtseva, T. K., Aguilera, V. M., Vodyanoy, I., Bezrukov, S. M., and Parsegian, V. A. (1998) *Biophys. J.* **75**, 1783–1792